

Episodic Evolution Mediates Interspecies Transfer of a Murine Coronavirus

RALPH S. BARIC,^{1,2*} BOYD YOUNT,¹ LISA HENSLEY,¹ SHEILA A. PEEL,¹ AND WAN CHEN¹

Program in Infectious Diseases, Department of Epidemiology, University of North Carolina at Chapel Hill, Chapel Hill, North Carolina 27599-7400,¹ and Department of Microbiology and Immunology, University of North Carolina at Chapel Hill, Chapel Hill, North Carolina 27599²

Received 21 May 1996/Accepted 11 November 1996

Molecular mechanisms permitting the establishment and dissemination of a virus within a newly adopted host species are poorly understood. Mouse hepatitis virus (MHV) strains (MHV-A59, MHV-JHM, and MHV-A59/MHV-JHM) were passaged in mixed cultures containing progressively increasing concentrations of non-permissive Syrian baby hamster kidney (BHK) cells and decreasing concentrations of permissive murine DBT cells. From MHV-A59/MHV-JHM mixed infection, variant viruses (MHV-H1 and MHV-H2) which replicated efficiently in BHK cells were isolated. Under identical treatment conditions, the parental MHV-A59 or MHV-JHM strains failed to produce infectious virus or transcribe detectable levels of viral RNA or protein. The MHV-H isolates were polytrophic, replicating efficiently in normally nonpermissive Syrian hamster smooth muscle (DDT-1), Chinese hamster ovary (CHO), human adenocarcinoma (HRT), primate kidney (Vero), and murine 17Cl-1 cell lines. Little if any virus replication was detected in feline kidney (CRFK) and porcine testicular (ST) cell lines. The variant virus, MHV-H2, transcribed seven mRNAs equivalent in relative abundance and size to those synthesized by the parental virus strains. MHV-H2 was an RNA recombinant virus containing a crossover site in the S glycoprotein gene. At the molecular level, episodic evolution and positive Darwinian natural selection were apparent within the MHV-H2 S and HE glycoprotein genes. These findings differ from the hypothesis that neutral changes are the predominant feature of molecular evolution and argue that changing ecologies actuate episodic evolution in the MHV spike glycoprotein genes that govern interspecies transfer and spread into alternative hosts.

Zoonotic viruses are potentially rich sources of new emerging viral diseases in humans and animals, yet the molecular and genetic mechanisms permitting the establishment and dissemination of such a virus within a newly adopted host are poorly understood (1, 2, 36, 39). While many suspect that most new viral diseases of humans arose by cross-species transmission from animal reservoirs, virology has largely remained outside the paradigm of the synthetic theory of evolution (34). Consequently, few studies have addressed at the molecular level the evolutionary mechanisms which contribute to the emergence and dissemination of new viral diseases in nature. This is unfortunate since evolution occurs at about 1 million-fold faster in RNA viruses than in their eukaryotic host counterparts, providing unparalleled power in studying fundamental principles in evolution (26).

Two principal mechanisms of evolution have been proposed at the molecular level. According to the more widely accepted neutral or nearly neutral theories (24, 27, 45), the majority of changes and polymorphisms at the molecular level result from the random fixation of selectively neutral or very nearly neutral mutations during continued pressure rather than by positive Darwinian natural selection. Since the majority of mutations are thought to be deleterious or lethal, silent substitution rates exceed replacement substitution rates because they are less subject to purifying selection. Mutation rates are believed to be relatively constant per generation, resulting in a near-constant molecular evolutionary clock, with functionally less important portions of genes evolving faster than more critical domains

(27, 45). In contrast, the episodic selection theory argues that molecular evolution is evolving in response to a slowly changing environment (20, 21). Rates of evolution increase during periods of environmental flux, negatively impacting progenitor viral quasispecies and selecting for the subsequent formation of new viral species (21). As environmental conditions change, previously deleterious alleles become more fit than the currently fixed alleles. The population evolves in short bursts by positive Darwinian selection at the molecular level, followed by longer periods of time with low levels of nucleotide substitution. Eldredge and Gould's theory of punctuated equilibrium (14), which was first used to explain phenotypic radiation during primate evolution, has more recently been used to explain the evolution and origin of human immunodeficiency virus (HIV) and simian immunodeficiency virus at the molecular level (1). Punctuated equilibrium, like Gillespie's episodic selection theory (20, 21), proposes that well-adapted populations maintain relatively low evolution rates until environmental conditions change, resulting in dramatic shifts in natural selection and accelerating rates of evolution. For uniformity, we will refer to these theories as episodic evolution.

Mouse hepatitis virus (MHV) and most other coronaviruses are extremely species and tissue specific *in vivo* and *in vitro* (28). Host range specificity is most likely mediated at entry since the MHV genomic RNA is infectious in nonpermissive cell lines (12, 13, 28). Expression of the MHV receptor, a biliary glycoprotein (Bgp1), converts nonpermissive Syrian baby hamster kidney (BHK), human, or primate cell lines into susceptible hosts for virus replication (12, 13). MHV contains a single-stranded positive-polarity RNA genome of about 32,000 nucleotides (nt) in length. The plasticity of the coronavirus genome is evidenced by high mutation ($\sim 10^{-4}$) and RNA recombination ($\sim 20\%$) rates, predicting a significant latent

* Corresponding author. Mailing address: Department of Epidemiology, University of North Carolina at Chapel Hill, Chapel Hill, NC 27599-7400. Phone: (919) 966-3895. Fax: (919) 966-2089.

capacity to evolve rapidly during periods of environmental flux (4, 18, 29, 33). In this report, we describe the isolation and characterization of host range mutants of MHV which replicate efficiently in normally nonpermissive BHK, Chinese hamster ovary (CHO), human, and primate cell lines. Given the nearly unprecedented transformation in the world's ecology, our findings suggest that RNA viruses demonstrating short generation times, high polymerase error, and high recombination rates may adapt rapidly by episodic evolution and positive Darwinian natural selection. The new viral forms surviving the period of adjustment to a new host may remodel those sites of virus-host interaction that initially enable broad-host-range interspecies transfer followed by subsequent speciation, dissemination, and emergence as new viral diseases in humans, animals, and plants.

MATERIALS AND METHODS

Virus strains and cell culture conditions. The MHV strains MHV-A59 and MHV-JHM were used throughout the course of these studies. Virus stocks were propagated in 150-cm² flasks containing DBT cells at 37°C, and titers were determined by plaque assay in DBT cells (4, 18). DBT cells were maintained at 37°C in Dulbecco's modified essential medium (DMEM) containing 6% fetal calf serum (FCS), 4% newborn calf serum, 5% tryptose phosphate broth (TPB), and 1% gentamicin-kanamycin (GIBCO). BHK cells were kindly provided by Robert E. Johnston (University of North Carolina) and propagated at 37°C in DMEM containing 10% FCS, 5% TPB, and 1% penicillin-streptomycin (GIBCO). DDT-1 cells, a Syrian hamster smooth muscle cell line, were propagated at 37°C in minimal essential medium (MEM) containing 10% FCS, 5% TPB, and 1% penicillin-streptomycin. CHO cells were maintained in MEM containing 10% FCS, 5% TPB, and 1% gentamicin-kanamycin at 37°C. Human adenocarcinoma (HRT) cells were kindly provided by Brenda Hogue (Baylor College of Medicine) and maintained at 37°C in DMEM-H (D-glucose; 4,500 ng/liter) containing 7% FBS, 10% TPB, and 1% penicillin-streptomycin. Porcine testicular (ST) cells were also provided by Brenda Hogue and maintained at 37°C in Eagle's MEM containing 10% FBS, 1× nonessential amino acids, and 1% penicillin-streptomycin. Feline kidney (CRFK) cells were kindly provided by Julie Levy, North Carolina State University, and were maintained at 37°C in DMEM-H containing 8% FCS and 1% gentamicin-kanamycin. African green monkey kidney (Vero) cells were maintained at 37°C in Eagle's MEM containing 10% FCS and 1% penicillin-streptomycin.

Selection for host range mutants. To select for host range mutants, MHV-A59, MHV-JHM, or an equal mix of both MHV-A59 and MHV-JHM was inoculated onto cultures containing 90% DBT and 10% BHK cells. Supernatants were harvested between 18 and 24 h postinfection, and the progeny virions were inoculated onto identical cultures of mixed cells. After ~5 serial passages under similar conditions, the concentrations of cells were adjusted in 10% increments until cultures eventually contained 10% DBT and 90% BHK cells. After 89 serial undiluted passages, viruses were isolated from the mixed MHV-A59/MHV-JHM-infected cultures, which replicated and produced syncytia in BHK cells. Since these variants could not be efficiently passaged in BHK cells, persistently infected BHK cells were established with the mixed MHV-A59/MHV-JHM passage 89 virus stocks. Persistently infected cultures were passaged at 3- to 5-day intervals for an additional 3 months. Virus variants (MHV-H1, MHV-H2, etc.) which replicated to high titer, produced syncytia within 36 to 48 h, and could be continuously passaged in BHK cells were subsequently isolated. Virus variants were plaque purified in BHK cells, individual plaques were purified again by plaque assay in DBT cells, and virus stocks were propagated in BHK cells for further use.

Virus growth curves and RNA synthesis. Cultures of BHK, DDT-1, CHO, 17Cl-1, HRT, Vero, CRFK, and ST cells in 60-mm² dishes were infected with MHV-A59, MHV-JHM, MHV-H1, or MHV-H2 at a multiplicity of infection (MOI) of 10. After 1 h at room temperature, the plates were washed twice with 4 ml of phosphate-buffered saline, overlaid with complete medium, and maintained at 37°C. Virus samples were harvested from supernatant culture fluids at the designated times, and virus growth curves were determined by plaque assay in DBT cells (4, 18). Intracellular RNA was also harvested from duplicate 60-mm² dishes, using RNA STAT-60 reagents as previously described (9).

To quantify levels of viral RNA, equivalent amounts of intracellular RNA (4.5 and 0.5 µg) were bound to nitrocellulose filters by using a Bio-Rad slot blot apparatus. The blots were hybridized with a radiolabeled MHV-H2 cDNA probe which spans nt 844 to 1415 in the N (nucleocapsid) gene (47). Briefly, the MHV-H2 N gene was cloned by reverse transcriptase PCR. cDNA was transcribed by using random primers and 200 U of Moloney murine leukemia virus reverse transcriptase (BRL) in a 20-µl reaction mixture containing 1 µg of MHV-H2 intracellular RNA, 4 µl of 5× first-strand reaction buffer (BRL), 2 µl of 0.1 M dithiothreitol (BRL), 1 µl of 10 mM deoxynucleoside triphosphate (Pharmacia), and 1 U of RNase inhibitor (Promega) for 1 h at 37°C. The cDNA

products were precipitated in ethanol and resuspended in 20 µl of deionized distilled H₂O. Forward (5'-CCAGTGCAGCAGTGT-3'; nt 844 to 860) and reverse-sense (5'-ACTTTCTCGGAGGGGTAC-3'; nt 1396 to 1415) oligonucleotide primer pairs were synthesized from highly conserved domains within the MHV N gene (47) and used for PCR amplification of a 571-nt MHV-H2 N gene DNA fragment. The DNA was inserted into pGEM-2, isolated after restriction digestion, and radiolabeled by using random primers and [³²P]dCTP. Blots were probed at 42°C in 50% formamide buffer containing 10 mM sodium phosphate buffer (pH 7.0), 5× Denhardt's solution (1× Denhardt's solution is 0.2 mg of Ficoll, 0.2 mg of polyvinylpyrrolidone, and 0.2 mg of bovine serum albumin per ml), and 100 µg of salmon sperm DNA per ml. The blots were washed twice at 65°C in 2× SSC (1× SSC is 0.15 M NaCl and 0.015 M sodium citrate) containing 0.2% sodium dodecyl sulfate (SDS), three times in 0.2× SSC containing 0.2% SDS, and twice in 0.2× SSC containing 0.1% SDS. The blots were dried and exposed to XAR-5 film with an intensifying screen and scanned by the AMBIS radioanalytic imaging system (RIS) (AMBIS, San Diego, Calif.).

Size analysis of MHV-H2 mRNAs. Viral RNAs were radiolabeled in 17Cl-1 or BHK cells. Cultures were seeded at densities of 3 × 10⁵ to 5 × 10⁵ cells per 35-mm² dish in 90% phosphate-free MEM containing 5% FCS and 3% newborn calf serum for 12 h. After infection with MHV-A59, MHV-JHM, MHV-H1, or MHV-H2, cultures were overlaid in 99% phosphate-free DMEM (pH 6.8) and incubated at 37°C. At the indicated times, the cultures were treated with actinomycin D (10 µg/ml) for 1 h and then radiolabeled with 300 µCi of [³²P]orthophosphate per ml for 1 h. The viral mRNAs were extracted and analyzed in 0.8% agarose gels containing Tris-borate-EDTA.

Cloning and sequencing the MHV-H2 genome. Intracellular RNA was isolated from MHV-H2-infected BHK cells at 24 h postinfection, using RNA STAT-60 reagents (total RNA/mRNA isolation reagent) as instructed by the manufacturer (Tel-Test "B", Inc.). To clone the MHV-H2 genome, several reverse transcriptase PCRs were performed with primer pairs located between open reading frame (ORF) 1b (nt 8015) and the HE gene (nt 891), nt 696 to 2080 in the HE gene, nt 1991 in HE to nt 669 in S, nt 629 to 2119 in S, nt 2066 to 4060 in S, nt 4041 in S to nt 536 in ORF 5B, nt 324 in ORF 5B to nt 476 in N, and nt 780 in M to nt 1415 in N (3, 31, 32, 47, 50, 54, 65, 66). Individual PCR products were isolated from agarose gels by using Qiagen reagents (Qiagen, Inc., Chatsworth, Calif.) and subcloned into TA cloning vectors (Promega). Positive clones were sequenced by the dideoxy method.

Statistical analysis and mutation rate calculations. Rates of mutation fixation per year as well as nonsynonymous and synonymous mutation rates per year were calculated as described previously (24, 26). All statistical tests were performed with EPI 6 software (Centers for Disease Control and Prevention, Atlanta, Ga.; World Health Organization, Geneva, Switzerland). Two-by-two contingency tests were used to compare the frequency of nucleotide changes relative to the size of a particular gene. Chi square or Fisher exact tests were used to determine if significantly different mutation rates per year were detected within different MHV-H2 genes or clusters of genes. Using the same approach, chi square or Fisher exact tests were used to determine if significantly different synonymous and nonsynonymous mutation fixation rates occurred within different portions of the MHV-H2 genome.

RESULTS

Isolation of MHV variants that bridge the species barrier. Because changing environmental niches appeared to favor the emergence and interspecies transfer of zoonotic pathogens in natural settings (36, 39), we passaged MHV in progressively decreasing concentrations of murine DBT cells (permissive) and progressively increasing concentrations of BHK cells (nonpermissive). BHK cells were chosen since MHV fails to enter or replicate in these nonpermissive cells (9, 12, 13), yet MHV-JHM causes receptor independent fusion between murine and BHK cell lines *in vitro* (19). This may enhance the opportunity for virus evolution and adaptation to hamster cell lines. MHV-A59, MHV-JHM, or an equal mix of both viruses was serially passaged in separate cultures containing 90% DBT and 10% BHK cells. Every ~5 passages, the concentrations of DBT and BHK cells were altered in 10% increments; i.e., virus from passage 5 was inoculated onto cultures containing 80% DBT and 20% BHK cells. Between passages 30 and 75, virus progeny were inoculated onto 70% BHK-30% DBT cell mixtures because inadequate virus replication was detected in higher ratios of BHK cells. After passage 75, the concentrations of cells was slowly adjusted to 90% BHK and 10% DBT cells over the next 14 passages. By passage 89, only the mixed MHV-A59/MHV-JHM inoculum caused significant syncytia (~50%) and cell death in 100% of BHK cells (Fig. 1). In contrast, only

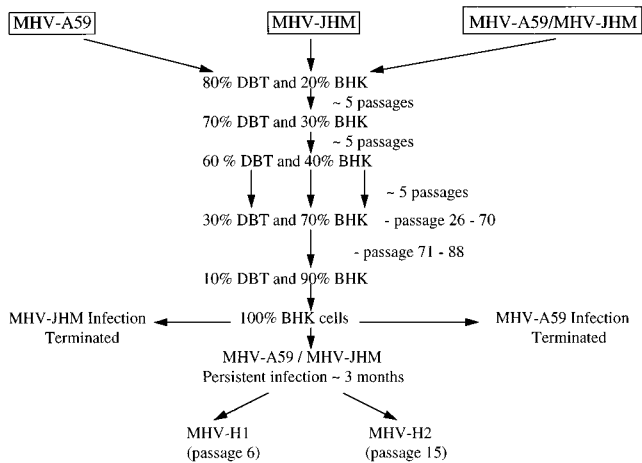


FIG. 1. Selection scheme for host range mutants of MHV in vitro.

minor amounts of cytopathic effect and viral RNA were detected in MHV-A59- or MHV-JHM-infected BHK cells (data not shown).

Since virus evolution is enhanced during persistent infection (9) and because the progeny from the passage 89 MHV-A59/MHV-JHM mixed infection were rapidly lost with serial passage in 100% of BHK cells, we continuously cultured the persistently infected BHK cell survivors. Low levels of infectious virus were detected for 3 months, at which time progeny virions were serially passaged 15 times in 100% BHK cells, demonstrating that MHV host range mutants had evolved (Fig. 1). Viruses from passages 6 (MHV-H1) and 15 (MHV-H2) were plaque purified in BHK cells, and stocks were propagated for use in subsequent experiments. The MHV-H variants were small-plaque mutants in both BHK and DBT cells. In DBT cells, the MHV-H2 variant produced plaques significantly smaller, 0.07 ± 0.02 mm, than the 0.24 ± 0.04 -mm plaques for MHV-A59 or MHV-JHM ($P < 0.001$). Interestingly, serial passage of MHV-A59 or MHV-JHM singly infected mixed cultures did not result in the emergence of isolates that bridged the species barrier.

Virus growth curves in murine and Syrian hamster cell lines. To characterize the host range phenotype of the MHV-H variants, cultures of 17Cl-1 (murine) and BHK cells were infected with MHV-A59, MHV-JHM, MHV-H1, or MHV-H2 at an MOI of 10 for 1 h at room temperature. The cultures were overlaid with medium, and virus samples were isolated at different times postinfection (Fig. 2). In 17Cl-1 cells, MHV-A59 and MHV-JHM replicated to titers approaching 10^8 and 10^7 , respectively. Under identical conditions of treatment, MHV-H1 and MHV-H2 replication was less efficient, with titers approaching $\sim 4 \times 10^6$. Both parental viruses, as well as the MHV-H variants, produced significant syncytia in 17Cl-1 cells within ~ 16 h postinfection. In agreement with previous studies, no MHV-A59 or MHV-JHM replication was detected in BHK cells (9, 13, 28). Under identical treatment conditions, however, both hamster-derived variants produced extensive syncytia and replicated to titers approaching 10^8 within 36 to 48 h postinfection. Using a polyclonal antiserum against MHV-3 and fluorescent antibody staining techniques, we determined that MHV-specific antigens were clearly present in the MHV-H2-infected BHK cultures but not in those infected with MHV-A59 or MHV-JHM (data not shown). These data

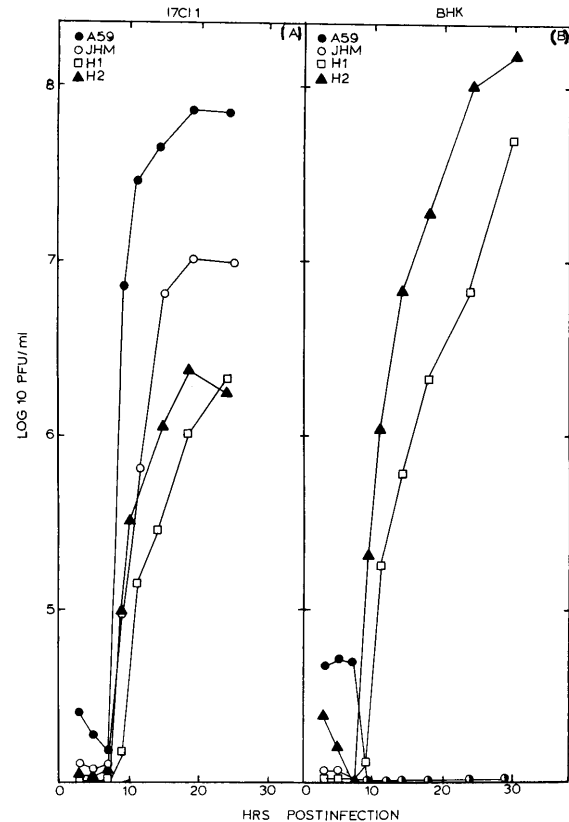


FIG. 2. Virus growth in murine and Syrian hamster cell lines. Cultures of 17Cl-1 and BHK cell lines containing 2×10^6 cells were infected with MHV-A59, MHV-JHM, MHV-H1, or MHV-H2 at an MOI of 10 for 1 h at room temperature. The inoculum was removed, the monolayers were washed twice, and samples were taken at the indicated times for plaque assay in DBT cells.

suggested that MHV-H2 was antigenically similar to MHV-A59 and MHV-JHM.

The MHV-H2 isolate was also more virulent in murine DBT and 17Cl-1 cells, resulting in $>99.998\%$ cell mortality in 30 h, compared with only $\sim 96.0\%$ cell mortality with MHV-A59 or MHV-JHM. MHV-H2 was also extremely cytolytic and destroyed over $>99.998\%$ of the BHK cell monolayer within 4 days postinfection. Under identical conditions, no BHK cell death was evident in MHV-A59- or MHV-JHM-infected cultures.

Viral RNA synthesis in 17Cl-1 and BHK cells. To provide additional evidence that the MHV-H2 variant virus replicated efficiently in 17Cl-1 and BHK cells, cultures were infected and intracellular RNA isolated at different times postinfection. Equivalent amounts of intracellular RNA were bound to nitrocellulose filters and probed with a PCR fragment spanning nt 844 to 1415 in the MHV-H2 N gene. The MHV-H2 probe detected MHV-A59 and MHV-H2 RNAs in 17Cl-1 cells, demonstrating that the MHV-H2 variant was closely related to the parental MHV strains (data not shown). The blots were scanned by AMBIS RIS, and levels of viral RNA were quantified and graphed (Fig. 3). Both parental viruses and MHV-H2 transcribed significant quantities of viral RNAs following infection of 17Cl-1 cells. Interestingly, while MHV-H2 replicated to lower titers than either of the parental viruses in 17Cl-1 cells, equivalent amounts of viral RNA were detected with this assay. Consistent with the ability to make infectious virus, only MHV-H2 synthesized significant quantities of viral

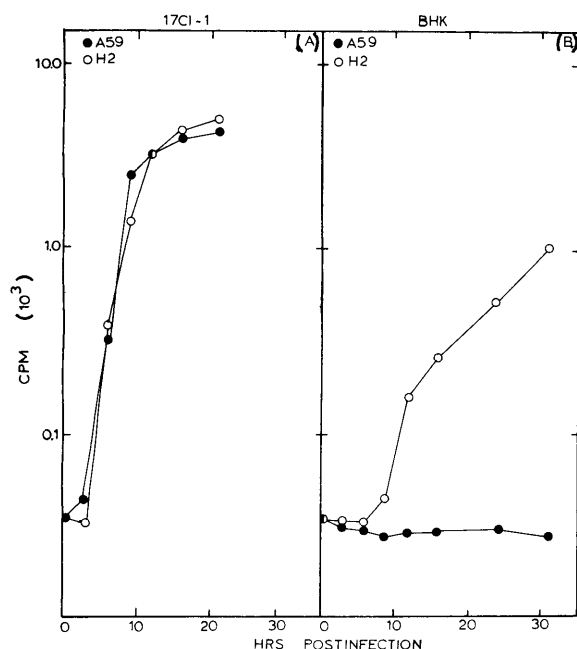


FIG. 3. Viral RNA synthesis in murine and Syrian hamster cell lines. Cultures of 17Cl-1 and BHK cell lines containing 2×10^6 cells were infected with MHV-A59 or MHV-H2 at an MOI of 10 for 1 h at room temperature. Intracellular RNA was isolated from the cells at the designated time points, equivalent amounts were bound to nitrocellulose filters and probed with an MHV-H2 N gene cDNA probe, and total counts per minute was quantified by AMBIS RIS.

RNA in BHK cells (Fig. 3). Similar findings were evident with MHV-H1 (data not shown).

Viral transcription in 17Cl-1 and BHK cells. To compare the quantities and sizes of the parental and hamster-adapted viral mRNAs, cultures of 17Cl-1 and BHK cells were infected with MHV-H2, MHV-H1, MHV-A59, or MHV-JHM and radiolabeled with [32 P]orthophosphate from 6 to 7 and 17 to 18 h postinfection, respectively. The different labeling periods reflected the delay in MHV-H2 replication seen in BHK cells compared with its replication in murine cell lines. After radiolabeling, intracellular RNA was isolated and separated on 0.8% agarose gels. Seven viral mRNAs were synthesized by MHV-H2 and the parental viruses in 17Cl-1 cells, although the sizes of MHV-H2 mRNAs 2 and 3 were more like those of MHV-JHM (Fig. 4A). Similar findings were noted with MHV-H1 (data not shown). Increased rates of transcription were also noted with MHV-H2 in 17Cl-1 cells compared to the parental controls. As expected, only the MHV-H variants transcribed detectable levels of viral mRNA in BHK cells (Fig. 4B). These results suggest that the MHV-H2 and MHV-H1 isolates are more homologous to MHV-JHM than MHV-A59, especially in the S and HE glycoprotein genes.

Host range specificity of the MHV-H2 isolate. Genetic alterations in the MHV-H variant viruses may have accorded a specific capacity to infect hamster cells or bestowed a broader host range specificity. To address this question, we analyzed the replication efficiencies of these viruses in various host species in vitro.

Cultures of cells were infected with MHV-A59 or MHV-H2, and virus titers and intracellular RNA were examined at different times postinfection. Not surprisingly, MHV-H2 replicated most efficiently in cell lines derived from *Mesocricetus auratus* (Syrian) hamsters (DDT-1) and *Cricetulus griseus* (Chinese) hamsters (CHO). In DDT-1 cells, MHV-H2 produced

significant syncytia by 30 h and reached titers approaching 10^8 PFU/ml within ~36 to 40 h postinfection. In CHO cells, the MHV-H2 replication cycle was completed within ~16 h, with titers approaching 10^7 PFU/ml (Fig. 5A). Significant amounts of syncytia were evident within ~8 to 12 h. The distinct rates of MHV-H2 replication and syncytium formation noted in different hamster and murine cell lines are intriguing and may reflect different rates of virus entry and uncoating. Consistent with the ability of MHV-H2 to produce infectious virus in both cell lines, significant quantities of viral RNA were also synthesized throughout infection (Fig. 5B). Under identical conditions, no evidence of parental virus replication or RNA synthesis was noted in either cell line.

Significant amounts of MHV-H2 replication were also evident in primate (Vero) and human (HRT) cell lines, with virus titers approaching $\sim 10^6$ PFU/ml within ~36 h postinfection (Fig. 6 and 7). Increased levels of MHV-H2 RNA synthesis were also evident in these cell lines (Fig. 6 and 7). Under identical treatment conditions, no parental MHV-A59 or MHV-JHM replication was apparent. These results indicated that genetic changes in the MHV-H2 genome have conferred a broad host range specificity. Since little virus replication and RNA synthesis were observed in ST (porcine) cells and no replication was evident in CRFK (feline) cells, specific host factors were still required to initiate a productive MHV-H2 infection (Fig. 6 and 7).

MHV-H2 genomic organization. To elucidate the molecular basis for MHV interspecies spread, we sequenced the 3'-most ~10 kb of the MHV-H2 genome (Fig. 8 and Table 1). MHV-H2 was an RNA recombinant virus containing a 5' end derived from MHV-JHM and a 3' end derived from MHV-A59. The crossover site in MHV-H2 resided between nt 3394 and 3417 within the ~4.1-kb S glycoprotein, effectively introducing nine MHV-A59 amino acid changes into the MHV-JHM S glycoprotein gene (32, 50). No amino acid changes were detected in the N gene, SM glycoprotein gene (ORF 5B), ORF 5A, or ORF 2 genetic domain, demonstrating that these loci do not encode critical determinants of interspecies spread (Fig. 8 and Table 1). No alterations were noted within the

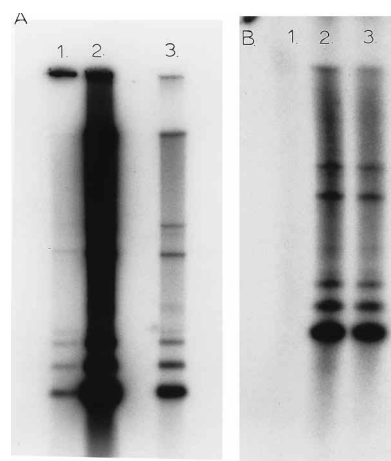


FIG. 4. Viral RNA synthesis in murine and hamster cell lines. Cultures of 17Cl-1 or BHK cells were infected with MHV-A59, MHV-JHM, MHV-H1, or MHV-H2 at an MOI of 10 for 1 h. The cultures were radiolabeled with 300 μ Ci of [32 P]orthophosphate per ml from 7 to 8 h postinfection in 17Cl-1 cells or 17 to 18 h postinfection in BHK cells. Intracellular RNA isolated and separated on 0.8% agarose gels. (A) 17Cl-1 cells infected with MHV-A59 (lane 1), MHV-H2 (lane 2), or MHV-JHM (lane 3); (B) BHK cells infected with MHV-A59 (lane 1), MHV-H2 (lane 2), or MHV-H1 (lane 3).

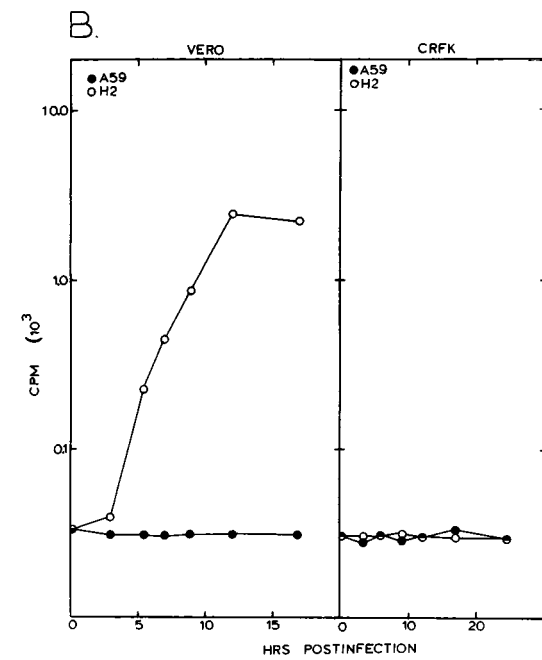
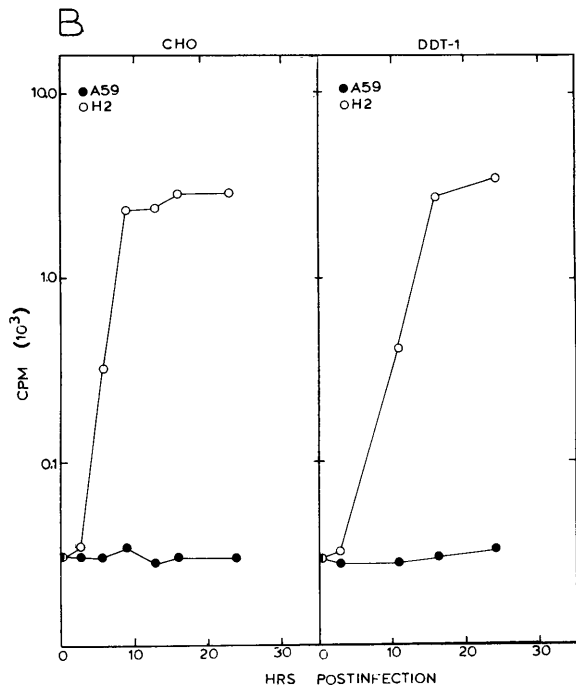
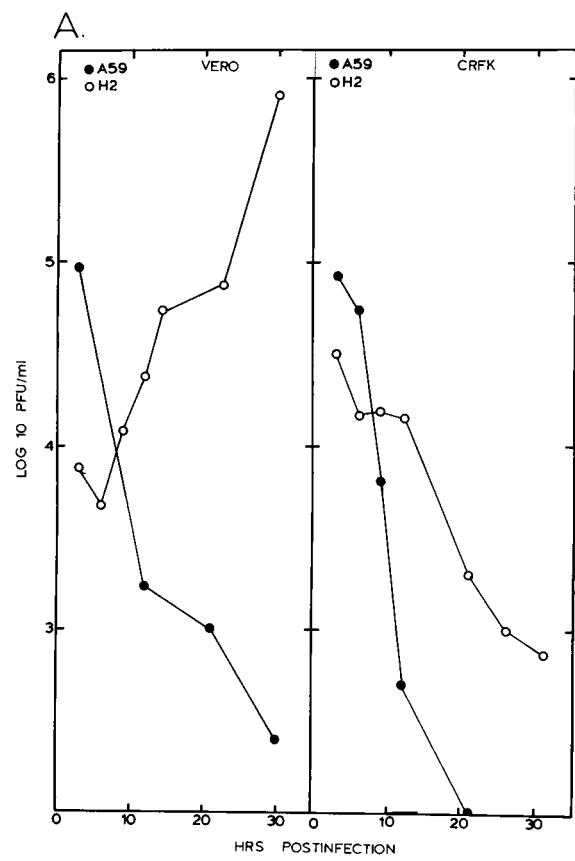
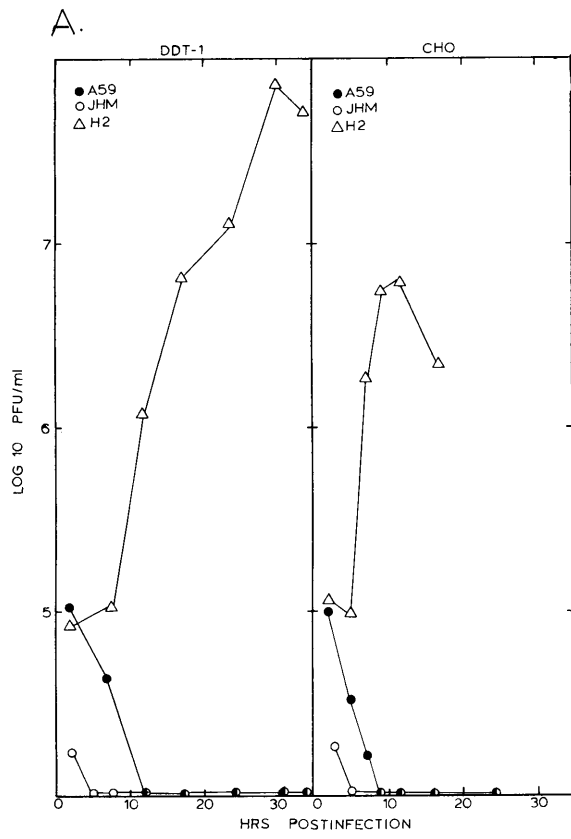


FIG. 5. Virus replication in Syrian and Chinese hamster cell lines. Cultures of Syrian hamster smooth muscle (DDT-1) or CHO cells were infected with MHV-A59 or MHV-H2 at an MOI of 10 for 1 h. The inoculum was removed, the monolayers were washed twice, and samples were taken at the indicated times for plaque assay in DBT cells. (A) Virus replication in DDT-1 and in CHO cells; (B) viral RNA synthesis in CHO and DDT-1 cells.

FIG. 6. Virus replication in primate and feline cell lines. Cultures of African green monkey kidney (Vero) and feline kidney (CRFK) cells were infected with MHV-A59 or MHV-H2 at an MOI of 10 for 1 h. The inocula were removed, the monolayers were washed twice, and samples were taken at the indicated times for plaque assay in DBT cells. (A) Virus replication in Vero and CRFK cells; (B) virus RNA synthesis in Vero and CRFK cells.

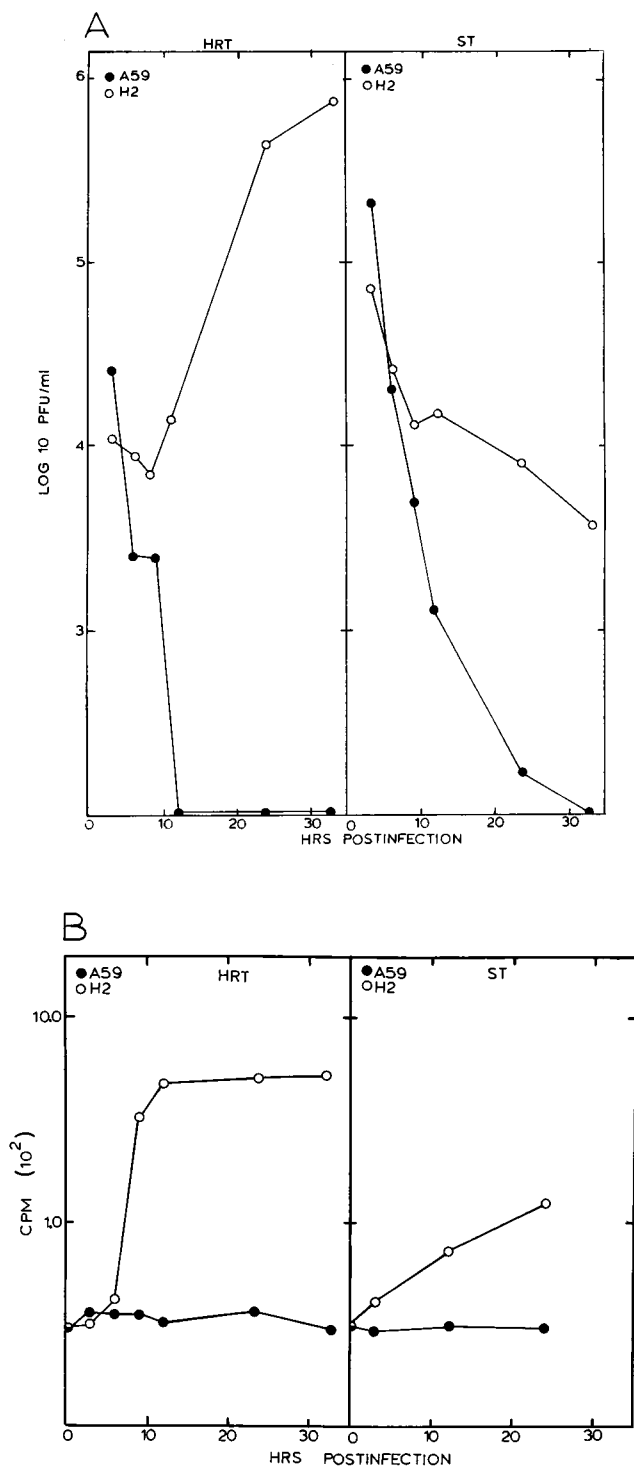


FIG. 7. Replication in human and porcine cell lines. Cultures of human adenocarcinoma (HRT) and porcine testicular (ST) cells were infected with MHV-A59 or MHV-H2 at an MOI of 10 for 1 h. The inoculum was removed, the monolayers were washed twice, and samples were taken at the indicated times for plaque assay in DBT cells. (A) Virus replication in HRT and ST cells; (B) virus RNA synthesis in HRT and ST cells.

MHV-H2 intergenic domains. A single C-terminal amino acid alteration was detected in the MHV-H2 M glycoprotein gene; this is an unlikely candidate for interspecies spread since it functions in assembly and release (3, 28). The amino acid 2

mutation in ORF 4 is also an unlikely candidate since it encodes a nonstructural protein which has been shown superfluous to productive viral infection (28, 65). Calculated mutation rates per site per year averaged $(3.84 \pm 2.25) \times 10^{-3}$ in the MHV-H2 N, M, ORF 5, ORF 4, and ORF 2 genetic domains.

The majority of amino acid alterations were detected within the MHV-H2 S and HE glycoprotein genes (Fig. 8). Overall, mutation rates in the MHV-H2 genome (including changes from recombination) were increased ~3.0- to 4.0-fold in the S and HE glycoprotein genes and averaged 16.13×10^{-3} and 10.85×10^{-3} per site per year, respectively. Using two-by-two contingency tests, we noted significant increases in the number of mutations within the MHV-H2 S ($\chi^2 = 13.88$, $P < 0.001$) and HE ($\chi^2 = 5.22$, $P < 0.03$) glycoprotein genes compared to the remaining subgenomic ORFs. In addition to the crossover site in the S glycoprotein gene, the region of polymorphism (nt 1359 to 1626) was extended by the removal of 12 additional amino acids (48), resulting in the insertion of an Arg residue. A 3-nt deletion between nt 2813 and 2815 resulted in the loss of position 938 proline. An additional eight mutations were noted in the S glycoprotein; six resulted in amino acid changes within the S1 domain, including a position 717 Arg-Gln change that resided within the S1-S2 protease cleavage site (25). Two additional amino acid changes were noted in S2. Rates of HE mutation fixation were increased about 2.6-fold compared to subgenomic ORFs which do not function in entry ($P < 0.03$). Interestingly, six of eight mutations resulted in amino acid changes (Table 1).

Evolutionary mechanisms for MHV-H2 interspecies transfer. Since MHV-H2 was derived from known progenitor strains over a 200-day period under clearly defined conditions of environmental flux, this biological model allowed us to elucidate the molecular evolutionary processes governing virus host range specificity *in vitro*. We have demonstrated an increased rate of evolution in the S and HE glycoprotein genes relative to evolution rates noted in viral genes that do not function in entry, suggesting that specific portions of the MHV-H2 genome may have evolved by episodic evolution. Overall rates of nonsynonymous mutations were also shown to be increased in the MHV-H2 attachment genes (HE and S) compared to the remaining subgenomic ORFs ($\chi^2 = 10.65$, $P < 0.002$) (Table 2). Individual increases in both the HE ($\chi^2 = 11.71$, $P < 0.001$) and S ($\chi^2 = 4.93$, $P < 0.03$) genes compared to rates in the remaining subgenomic ORFs were noted (Table 2). Inclusion of the 12-amino-acid deletion noted in the region of S gene polymorphism resulted in even greater statistical significance ($\chi^2 = 18.11$, $P < 0.001$) in the nonsynonymous mutation rate. Importantly, no synonymous mutations were detected within the MHV-H2 S gene, and only two of eight mutations were synonymous in HE (Tables 1 and 2). In contrast, viral genes which did not function in entry demonstrated near genetic stasis, with synonymous changes predominating (Tables 1 and 2). Since neither lineage effects nor neutral theory could account for the evolutionary pulse or the increased rate of nonsynonymous mutations detected within the MHV-H2 HE and S genes, episodic evolution and positive Darwinian selection at the molecular level likely modulated interspecies transfer *in vitro* (14, 20, 21).

DISCUSSION

Virus interspecies traffic. Animal virus host range specificity and the evolution of new viral diseases are complex phenomena involving interactions between the virus, the host, and the environment. Emerging viruses are frequently defined as either newly recognized viruses or viral pathogens that are rapidly

TABLE 1. Locations of synonymous and nonsynonymous mutations in the MHV-H2 genome

Viral gene	Mutation	nt position	Amino acid
N gene	A-T	69	No change
	T-A	441	No change
	T-C	612	No change
M gene	G-A	103	No change
	C-T	541	No change
	T-C	759	Ile-Thr
ORF 5A	G-T	18	Noncoding
ORF 5B			No change
ORF 4	G-T	88	Val-Leu
S gene ^a	C-T	520	Val-Leu
	CTG-GCT	763-765	Leu-Ala
	C-A	842	Ala-Val
	A-G	1205	Asp-Gly
	CGC ^b		Arg ^b
	A-C	1849	Asn-His
	G-A	2150	Arg-Gln
	A-G	2696	Glu-Gly
	CCA ^c	2812-2814	Del Pro ^c
	G-T	3448	Asp-Tyr
	HE gene	T-C	926
T-G		996	Val-Gly
C-A		1104	Asp-Lys
T-C		1122	No change
T-C		1421	Val-Ala
G-C		1497	No change
G-C		1596	Leu-Phe
G-C		1601	Cys-Ser
T-C		285	No change
ORF 2			No change

^a Does not include the 9-nt differences from MHV-A59.

^b Resulting from the deletion in viral amino acids 445 to 546.

^c Resulting from a 3-nt deletion in the S gene sequence.

cells do not evolve the capacity to replicate in hamster cell lines in vitro (9), it seems likely that the MHV-H host range variants evolved in response to the presence of increasing concentrations of BHK cells. Efficient MHV-H adaptation and replication, however, were not accomplished until a persistent infection was established in hamster cell lines. Although the mechanism is speculative, persistent infection may have selected not only for the emergence of resistant host cells that expressed little receptor protein but also for the subsequent coevolution of more virulent virus variants that recognized alternative receptors for entry (9).

Interestingly, serial passage of singly infected MHV-A59 and MHV-JHM cultures did not result in the emergence of isolates that replicated efficiently in hamster cell lines. While these findings do not imply that host range mutants of MHV-A59 or MHV-JHM cannot evolve under continued selection, mechanistically, rapid evolution in the MHV-H2 S glycoprotein gene was primarily driven by RNA recombination. These findings suggest that RNA recombination maximizes the rate at which genetic variability accumulates in viral genes critical for host range specificity (16, 28). In support of this hypothesis, type-specific oligonucleotide probes demonstrated that at least five other MHV-H isolates were recombinant viruses containing a genome organization like MHV-H2 (data not shown). The increased MHV-H virulence in vitro may also reflect a serious consequence of recombination and cross-species transmission of zoonotic viruses in nature, an extremely cytolytic course of infection in the adopted host (15). For example, simian immunodeficiency virus infection is extremely cytolytic in human cell lines yet produces a noncytolytic infection in the natural host (1).

Our in vitro model likely reflects mechanisms of virus adaptation associated with mixed cell populations in vivo; similar conditions are present in humans following xenotransplantation. Mystery virus adaptation to the human host may be a concern in xenotransplant recipients (35). Although speculative, our findings suggest that heavily immunosuppressed xenograph recipients may represent an ideal environment for rapid zoonotic virus adaptation and dissemination into the human host.

Mechanisms of MHV interspecies transfer. Selection for efficient MHV replication in BHK cells resulted in variants with polytrophic host range phenotypes. In vivo examples of similar phenomena include influenza virus (H1N1) in swine, and the avian-derived 1979-1980 seal influenza virus (H7N7), which also caused conjunctivitis in humans (23, 52, 53, 62). While the natural reservoir of equine morbillivirus is unknown, zoonotic transfer resulted in increased morbidity and mortality in both equine and human hosts (40). These examples suggest that interspecies transfer of viruses may evolve by changes which confer broad host range specificity, followed by adaptation and speciation within a particular host.

MHV-H2 has likely remodeled its normal interactions with cellular receptors. Although we cannot exclude the possibility that mutations in the ORF 1a or ORF 1b polymerase gene may have contributed to MHV-H2 replication, the sequence data suggest that the HE and S glycoprotein genes represent the principal genetic determinants mediating interspecies traffic of coronaviruses. While the MHV HE glycoprotein is not required for entry (31, 66), the MHV-H2 HE may now function like the bovine coronavirus HE glycoprotein and recognize neuramic acid residues on cellular proteins as receptors for entry (28, 60). Alternatively, the S glycoprotein gene interacts with the murine Bgp glycoprotein receptor (12, 13, 57, 66). Since human, rat, and murine Bgps are highly conserved in nature and vary by 60 to 90% at the amino acid level (30), this model may reveal whether phylogenetic homologs of the normal receptor function as natural conduits for interspecies traffic of coronaviruses.

Interspecies transfer and coronavirus evolution. Phylogenetic analysis of the group II coronaviruses have predicted two clades, one containing bovine coronavirus and HCV-OC43 and the other containing MHV and rat coronaviruses (37, 38, 67). Comparisons of sequences among the viruses indicate that the N and M structural proteins are most highly conserved, with the greatest sequence diversity evident in the S and HE glycoprotein genes. In the S gene, the greatest heterogeneity is detected within the S1 domain (31, 32, 37, 38, 48, 67). These

TABLE 2. Fixation rates of synonymous and nonsynonymous substitutions for MHV-H2 genes

Viral gene(s)	No. of substitutions/site/yr ^a	
	Synonymous	Nonsynonymous
S/HE	6.75×10^{-4}	4.72×10^{-3}
M, N, 5AB, 4, 2	2.92×10^{-3}	8.36×10^{-4}
HE	2.70×10^{-3}	8.13×10^{-3}
S	0	3.59×10^{-3}
N	3.29×10^{-3}	0
M	4.67×10^{-3}	2.43×10^{-3}
5AB	2.70×10^{-3}	0
4	0	4.40×10^{-3}
2	2.17×10^{-3}	0

^a Does not include alterations resulting from recombination and deletion.

findings may reflect evolutionary patterns detected in the MHV-H2 genome and suggest that the increased heterogeneity noted in the HE and S genes in the group II coronaviruses was partially a consequence of interspecies transfer and adaptation to new host species. Importantly, the S and HE glycoprotein genes of MHV-H2 contain less sequence variation than that noted among different MHV strains in nature (31, 32, 48, 66). These findings suggest that a relatively few amino acid alterations are needed to alter species specificity in coronaviruses.

Beyond the generalized interpretation that mutations in the MHV-H2 HE and S glycoprotein have expanded host range specificity, no predictions can be made concerning the importance of individual mutations in this process. Certainly mutations likely function in the establishment and maintenance of MHV persistence in BHK cells or alter virus fusion, virulence, or cell cytopathic effects in vitro. For example, a position 717 Arg-Gln change within the S1-S2 putative host protease cleavage site likely evolved as a consequence of persistence and functions to decrease the rate of MHV-H2-induced fusion. Similar mutations have been detected during persistent MHV infection in murine cell lines (25). The MHV-H variants should provide a means to identify virus residues that bind with cellular receptor proteins and permit the identification of host receptor protein residues that bind virus to initiate a productive infection in different species.

Evolutionary mechanisms of virus interspecies spread. While the neutral or nearly neutral allele theories have successfully accounted for many of the evolutionary phenomena observed at the molecular level (24, 27, 45), a number of findings have suggested that natural selection may also shape the genetic structure of populations (20, 21). In support of neutral theory, sequence analyses of many RNA and DNA viruses have demonstrated that the accumulation of synonymous substitutions is about three- to fivefold higher than the rate for nonsynonymous substitutions and also revealed that many viral evolutionary clocks appear somewhat constant (24). In contrast, eastern equine encephalitis virus has displayed little genetic change over the past 50 years despite a prediction of high mutation frequency (61). In addition, several reports have demonstrated the accumulation of nonsynonymous substitutions during RNA virus or retrovirus evolution (8, 11). Episodic selection theory proposes that molecular evolution may be limited by the rate of change in the environment, with one or more loci evolving by natural selection, genetic drift, and mutation in response to these changing conditions. Influenza A viruses have probably evolved by positive Darwinian selection in response to host immune selection because hemagglutinins evolved more rapidly than nonstructural genes and fixed proportionately more nonsynonymous mutations in antigenic sites in survivors than in nonsurvivors (17). Molecular evolution in the P gene of vesicular stomatitis virus correlates with a south-to-north geographic migration and is more consistent with episodic evolution and positive Darwinian selection (44).

The extraordinarily high mutation rates seen in the MHV-H2 S and HE glycoprotein genes (Table 2) are comparable with rates observed in HIV and influenza virus except that the majority of MHV-H2 mutations result in nonsynonymous changes. Although other mechanisms may also account for the emergence of new viral diseases in nature, our findings are most consistent with Gillespie's episodic selection theory since nonsynonymous mutations predominate and lineage effects could not account for the evolutionary pulse detected in these genes (14, 20, 21). In contrast to neutral theory, our findings also suggest that natural selection may actually in-

crease the evolution rates in functionally more important genetic domains such as receptor binding residues, thereby permitting more rapid viral adaptation, entry, and survival within alternative hosts. While neutral theory could explain the evolutionary changes seen in those MHV genes which did not function in entry, positive Darwinian natural selection in the S and HE glycoprotein genes was probably the principal force driving the adaptation of MHV-H2 to hamster cell lines. Unfortunately, theories explaining evolutionary change and polymorphism by natural selection are not as well developed as neutral theory because of the inherent difficulties in modeling ecosystems and identifying the targets of selection at the molecular level (20, 21). More model systems are needed to determine whether neutral evolution is an important evolutionary phenomena or represents, as suggested by some naturalists, little more than evolutionary noise (34).

ACKNOWLEDGMENTS

This research was supported by grant AI23946 from the National Institutes of Health and was performed during the tenure of an Established Investigator Award of the American Heart Association (AHA 89-0193) (R.S.B.). Wan Chen was supported by postdoctoral fellowship 5 T32 A107151-16 from the National Institutes of Health.

REFERENCES

- Allan, J. S. 1992. Viral evolution and AIDS. *J. NIH Res.* **4**:51-54.
- Ampel, N. M. 1991. Plagues—what's past is present: thoughts on the origin and history of new infectious diseases. *Rev. Infect. Dis.* **13**:658-665.
- Armstrong, J., H. Niemann, S. Smeekens, P. Rottier, and G. Warren. 1984. Sequence and topology of a model intracellular membrane protein, E1 glycoprotein, from a coronavirus. *Nature* **308**:751-752.
- Baric, R. S., K. S. Fu, M. C. Schaad, and S. A. Stohman. 1990. Establishing a genetic recombination map for MHV-A59 complementation groups. *Virology* **177**:646-656.
- Bridgen, A., M. Duarte, K. Tobber, H. Laude, and M. Ackermann. 1993. Sequence determination of the nucleocapsid gene of a porcine epidemic diarrhoea virus confirms that it is closely related to human coronavirus 229E and TGEV. *J. Gen. Virol.* **74**:1795-1804.
- Brown, E. G. 1990. Increased virulence of a mouse-adapted variant of influenza A/FM/1/47 virus is controlled by mutations in genome segments 4, 5, 7, and 8. *J. Virol.* **64**:4523-4533.
- Burks, J. S., B. L. Pelletier, V. Calvez, and F. Colbere-Garapin. 1980. Two coronaviruses isolated from central nervous system tissue of two multiple sclerosis patients. *Science* **209**:933-934.
- Burns, D. P. W., and R. C. Desrosiers. 1991. Selection of genetic variants of simian immunodeficiency virus in persistently infected rhesus monkeys. *J. Virol.* **65**:1843-1854.
- Chen, W., and R. S. Baric. 1996. Molecular anatomy of MHV persistence: coevolution of increased host resistance and virus virulence. *J. Virol.* **70**:3947-3960.
- Clarke, D. K., E. A. Duarte, A. Moya, S. F. Elena, E. Domingo, and J. Holland. 1993. Genetic bottlenecks and population passages cause profound fitness differences in RNA viruses. *J. Virol.* **67**:222-228.
- Diez, J., M. Davila, C. Escarmis, M. G. Mateu, J. Dominguez, J. J. Perez, E. Giral, J. A. Melero, and E. Domingo. 1990. Unique amino acid substitutions in the capsid proteins of foot-and-mouth disease virus from a persistent infection in cell culture. *J. Virol.* **60**:5519-5528.
- Dveksler, G. S., C. W. Pensiero, C. B. Cardellicchio, K. McCuaig, M. N. Pensiero, G.-S. Jiang, N. Beauchemin, and K. V. Holmes. 1993. Several members of the mouse carcinoembryonic antigen-related glycoprotein family are functional receptors for the coronavirus mouse hepatitis virus-A59. *J. Virol.* **67**:1-8.
- Dveksler, G. S., M. N. Pensiero, C. B. Cardellicchio, R. K. Williams, G.-S. Jiang, K. V. Holmes, and C. W. Dieffenbach. 1991. Cloning of the mouse hepatitis virus (MHV) receptor: expression in human and hamster cell lines confers susceptibility to MHV. *J. Virol.* **65**:6881-6891.
- Eldredge, N., and S. J. Gould. 1977. Punctuated equilibria: an alternative phyletic gradualism, p. 82-115. *In* T. J. M. Schopf (ed.), *Models in paleobiology*. Freeman and Cooper, San Francisco, Calif.
- Ewald, P. W. 1990. Transmission modes and the evolution of virulence. *Hum. Nat.* **2**:1-30.
- Fernandez-Cuartero, B., J. Burgyan, M. A. Aranda, K. Salanki, E. Moriones, and F. Garcia-Arenal. 1994. Increase in the relative fitness of a plant virus RNA associated with its recombinant nature. *Virology* **203**:373-377.
- Fitch, W. M., J. M. E. Leiter, X. Li, and P. Palese. 1991. Positive Darwinian evolution in human influenza A virus. *Proc. Natl. Acad. Sci. USA* **88**:4270-4274.

18. **Fu, K., and R. S. Baric.** 1994. Map locations of mouse hepatitis virus temperature sensitive mutants: confirmation of variable rates of recombination. *J. Virol.* **68**:7458–7466.
19. **Gallagher, T. M., M. J. Buchmeier, and S. Perlman.** 1992. Cell receptor independent infection by a neurotropic coronavirus. *Virology* **91**:517–522.
20. **Gillespie, J. H.** 1995. On Ohta's hypothesis: most amino acid substitutions are deleterious. *J. Mol. Evol.* **40**:64–69.
21. **Gillespie, J. H.** 1984. The molecular clock may be an episodic clock. *Proc. Natl. Acad. Sci. USA* **81**:8009–8013.
22. **Gammel, M., A. Altmüller, U. Reinhardt, J. Mandler, V. R. Harley, P. J. Hudson, W. M. Fitch, and C. Scholtissek.** 1990. Phylogenetic analysis of nucleoprotein suggests that human influenza A virus emerged from a 19th Century avian ancestor. *Mol. Biol. Evol.* **7**:194–200.
23. **Geraci, J. R., D. J. Aubin, and L. K. Baker.** 1982. Mass mortality of harbor seals: pneumonia associated with influenza A virus. *Science* **215**:1129–1131.
24. **Gojobori, T., E. N. Moriyama, and M. Kimura.** 1990. Molecular clock of viral evolution, and the neutral theory. *Proc. Natl. Acad. Sci. USA* **87**:10015–10018.
25. **Gombold, J. E., S. T. Thingley, and S. R. Weiss.** 1993. Fusion defective mutants of mouse hepatitis virus A59 contain a mutation in the spike protein cleavage signal. *J. Virol.* **67**:4504–4512.
26. **Holland, J. J., J. C. De La Torre, and D. A. Steinhauer.** 1992. RNA virus populations as quasispecies. *Curr. Top. Microbiol. Immunol.* **176**:1–43.
27. **Kimura, M.** 1989. The neutral theory of molecular evolution and the world view of the neutralists. *Genome* **31**:24–31.
28. **Lai, M. M. C.** 1990. Coronaviruses: organization, replication and expression of genome. *Annu. Rev. Microbiol.* **44**:303–333.
29. **Lai, M. M. C.** 1992. Genetic recombination in RNA viruses. *Curr. Top. Microbiol. Immunol.* **176**:21–32.
30. **Lin, S.-H., and G. Guidotti.** 1989. Cloning and expression of a cDNA coding for a rat liver plasma membrane ecto-ATPase. The primary structure of the ecto-ATPase is similar to that of the human biliary glycoprotein I. *J. Biol. Chem.* **264**:14408–14414.
31. **Luytjes, W., P. J. Bredenbeek, A. F. H. Noten, M. C. Horzinek, and W. J. M. Spaan.** 1988. Sequence of mouse hepatitis virus A59 mRNA 2: indications for RNA recombination between coronavirus and influenza C virus. *Virology* **166**:415–422.
32. **Luytjes, W., P. J. Bredenbeek, J. Charite, B. A. van der Zeijst, M. C. Horzinek, and W. J. Spaan.** 1987. Primary structure of the glycoprotein E2 of coronavirus MHV-A59 and identification of the trypsin cleavage site. *Virology* **161**:479–487.
33. **Makino, S., J. G. Keck, S. A. Stohman, and M. M. C. Lai.** 1986. High frequency RNA recombination of murine coronaviruses. *J. Virol.* **57**:729–737.
34. **Mayer, E.** 1994. Driving forces in evolution. An analysis of natural selection, p. 29–48. *In* S. S. Morse (ed.), *The evolutionary biology of viruses*. Raven Press, New York, N.Y.
35. **Michler, R. E.** 1996. Xenotransplantation: risks, clinical potential and future prospects. *Emerging Infect. Dis.* **2**:64–70.
36. **Morse, S. S., and A. Schluenderberg.** 1990. Emerging viruses: the evolution of viruses and viral diseases. *J. Infect. Dis.* **162**:1–15.
37. **Mounir, S., and P. J. Talbot.** 1992. Sequence analysis of the membrane protein gene of human coronavirus OC43 and evidence of O-glycosylation. *J. Gen. Virol.* **73**:2731–2736.
38. **Mounir, S., and P. J. Talbot.** 1993. Molecular characterization of the S protein gene of human coronavirus. *J. Gen. Virol.* **74**:1981–1989.
39. **Murphy, F. A.** 1994. New emerging and reemerging infectious diseases. *Adv. Virus Res.* **43**:1–52.
40. **Murray, K., P. Selleck, P. Hooper, A. Hyatt, A. Gould, L. Gleeson, H. Westbury, L. Hiley, L. Selvey, B. Rodwell, and P. Ketterer.** 1995. A morbillivirus that caused fatal disease in horses and humans. *Science* **268**:94–97.
41. **Murray, M. G., J. Bradley, X.-F. Yang, E. Wimmer, E. G. Moss, and V. R. Racaniello.** 1988. Poliovirus host range is determined by a short amino acid sequence in neutralization antigenic site I. *Science* **241**:213–215.
42. **Murray, R. S., B. Brown, D. Brian, and G. F. Gabirac.** 1992. Detection of coronavirus RNA and antigen in multiple sclerosis brain. *Ann. Neurol.* **31**:525–533.
43. **Murray, R. S., G.-Y. Cal, K. Hoel, J.-Y. Zhang, K. F. Soike, and G. F. Cabirac.** 1992. Coronavirus infects and causes demyelination in the primate central nervous system. *Virology* **188**:274–284.
44. **Nichol, S. T., J. D. Rowe, and W. M. Fitch.** 1993. Punctuated equilibrium and positive Darwinian evolution in vesicular stomatitis virus. *Proc. Natl. Acad. Sci. USA* **90**:10424–10428.
45. **Ohta, T.** 1995. Synonymous and nonsynonymous substitutions in mammalian genes and the nearly neutral theory. *J. Mol. Evol.* **40**:56–63.
46. **Parish, C. R.** 1994. The emergence and evolution of canine parvovirus—an example of recent host range mutation. *Semin. Virology* **5**:121–132.
47. **Parker, M. M., and P. S. Masters.** 1990. Sequence comparison of the N genes of five strains of the coronavirus mouse hepatitis virus suggests a three domain structure for the nucleocapsid protein. *Virology* **179**:463–468.
48. **Parker, S. E., T. M. Gallagher, and M. J. Buchmeier.** 1989. Sequence analysis reveals extensive polymorphism and evidence of deletions within the E2 glycoprotein gene of several strains of murine hepatitis virus. *Virology* **173**:664–673.
49. **Rasschaert, D., M. Duarte, and H. Laude.** 1990. Porcine respiratory coronavirus differs from transmissible gastroenteritis virus by a few genomic deletions. *J. Gen. Virol.* **71**:2599–2607.
50. **Schmidt, I., M. A. Skinner, and S. G. Siddell.** 1987. Nucleotide sequence of the gene encoding the surface projection glycoprotein of coronavirus MHV-JHM. *J. Gen. Virol.* **68**:47–56.
51. **Scholtissek, C., I. Koennecke, and R. Rott.** 1978. Host range recombinants of fowl plaque (influenza A) virus. *Virology* **91**:79–85.
52. **Shope, R. E.** 1931. Swine influenza. III. Filtration experiments and etiology. *J. Exp. Med.* **54**:373–380.
53. **Shope, R. E.** 1958. Swine influenza, p. 81–91. *In* H. W. Dunne (ed.), *Diseases of swine*, 1st ed. Iowa State University Press, Ames.
54. **Skinner, M. A., D. Ebner, and S. G. Siddell.** 1985. Coronavirus MHV-JHM mRNA 5 has a sequence arrangement which potentially allows translation of a second, downstream open reading frame. *J. Gen. Virol.* **66**:581–592.
55. **Stewart, J. N., S. Mounir, and P. J. Talbot.** 1992. Human coronavirus gene expression in the brains of multiple sclerosis patients. *Virology* **191**:502–505.
56. **Subbarao, E. K., W. London, and B. R. Murphy.** 1993. A single amino acid in the PB2 gene of influenza A virus is a determinant of host range. *J. Virol.* **67**:1761–1764.
57. **Suzuki, H., and F. Taguchi.** 1996. Analysis of the receptor binding site of murine coronavirus spike glycoprotein. *J. Virol.* **70**:2632–2636.
58. **Tian, S.-F., A. J. Buckler-White, W. T. London, L. J. Reck, R. M. Chanock, and B. R. Murphy.** 1985. Nucleoprotein and membrane protein genes are associated with restriction of replication of influenza A/Mallard?NY/78 virus and its reassortants in squirrel monkey respiratory tract. *J. Virol.* **53**:771–775.
59. **Truyen, U., J. F. Evermann, E. Vieler, and C. R. Parrish.** 1996. Evolution of canine parvovirus involved loss and gain of feline host range. *Virology* **215**:186–189.
60. **Vlasak, R., W. Luytjes, W. J. M. Spaan, and P. Palese.** 1988. Human and bovine coronaviruses recognize sialic acid containing receptors similar to those of influenza viruses. *Proc. Natl. Acad. Sci. USA* **85**:4526–4529.
61. **Weaver, S. C., T. W. Scott, and R. Rico-Hesse.** 1991. Molecular evolution of eastern equine encephalomyelitis virus in North America. *Virology* **182**:774–781.
62. **Webster, R. G., J. R. Geraci, G. Petrusson, and K. Skirnmision.** 1981. Conjunctivitis in human beings caused by influenza A virus of seals. *N. Engl. J. Med.* **304**:911–914.
63. **Wimmer, E.** 1994. Cellular receptors for viruses, p. 1–14. *In* E. Wimmer (ed.), *Cellular receptors for viruses*. Cold Spring Harbor Laboratory Press, Plainview, N.Y.
64. **Yin, F. H., and N. B. Lomax.** 1983. Host range mutants of human rhinoviruses in which nonstructural genes are altered. *J. Virol.* **48**:410–418.
65. **Yokomori, K., and M. M. C. Lai.** 1991. Mouse hepatitis virus S RNA sequence reveals that nonstructural proteins ns4 and ns5a are not essential for murine coronavirus replication. *J. Virol.* **65**:5605–5608.
66. **Yokomori, K., L. R. Banner, and M. M. C. Lai.** 1991. Heterogeneity of gene expression of the hemagglutinin-esterase (HE) protein of murine coronaviruses. *Virology* **183**:647–657.
67. **Zhang, X., K. G. Kousoulas, and J. Storz.** 1992. The hemagglutinin gene of human coronavirus OC43: Phylogenetic relationships to bovine and murine coronaviruses and influenza C virus. *Virology* **180**:221–228.